IRIS AperTO

UNIVERSITÀ DEGLI STUDI DI TORINO

AperTO - Archivio Istituzionale Open Access dell'Università di Torino

IL-17A Is Increased in Humans with Primary Hyperparathyroidism and Mediates PTH-Induced Bone Loss in Mice

This is the author's manuscript

Original Citation:

Availability:

This version is available http://hdl.handle.net/2318/1535758 since 2016-09-14T12:47:43Z

Published version:

DOI:10.1016/j.cmet.2015.09.012

Terms of use:

Open Access

Anyone can freely access the full text of works made available as "Open Access". Works made available under a Creative Commons license can be used according to the terms and conditions of said license. Use of all other works requires consent of the right holder (author or publisher) if not exempted from copyright protection by the applicable law.

(Article begins on next page)

07 January 2023

UNIVERSITÀ DEGLI STUDI DI TORINO

***This is an author version of the contribution published on**:*
Questa è la versione dell'autore dell'opera:
IL-17A IS INCREASED IN HUMANS WITH PRIMARY HYPERPARATHYROIDISM AND MEDIATES PTH-INDUCED BONE LOSS IN MICE

Li JY, D'Amelio P, Robinson J, Walker LD, Vaccaro C, Luo T, Tyagi AM, Yu M, Reott M, Sassi F, Buondonno I, Adams J, Weitzmann MN, Isaia GC, Pacifici R.

*Cell Metab. 2015 Nov 3;22(5):799-810. doi: 10.1016/j.cmet.2015.09.012..**The definitive version is available at:***
La versione definitiva è disponibile alla URL:
[http://www.sciencedirect.com/science/article/pii/S1550413115004696]

IL-17A IS INCREASED IN HUMANS WITH PRIMARY HYPERPARATHYROIDISM AND MEDIATES PTH-INDUCED BONE LOSS IN MICE

Jau-Yi Li*1, Patrizia D'Amelio*2, Jerid Robinson1, Lindsey D. Walker1, Chiara Vaccaro1, Tao Luo1, Abdul Malik Tyagi1, Mingcan Yu1, Michael Reott1, Francesca Sassi2, Ilaria Buondonno2, Jonathan Adams1, M. Neale Weitzmann1,3, Giovanni Carlo Isaia2, and Roberto Pacifici1,4

* These authors have contributed equally

1Division of Endocrinology, Metabolism and Lipids, Department of Medicine, Emory University,
Atlanta, GA, 2Gerontology Section, Department of Medical Sciences, University of Torino, Corso
Bramante 88/90, 10126 Torino, Italy, 3Atlanta Department of Veterans Affairs Medical Center,
Decatur, GA 30033, 4Immunology and Molecular Pathogenesis Program, Emory University,
Atlanta, GA.

Key Words: PTH, Hyperparathyroidism, T cells, Th17 cells, IL-17, IL-17R, IL-17 antibody,
bone

Running title: IL-17A mediates PTH induced bone loss

Nonstandard abbreviations used: Bone marrow (BM), Continuous PTH (cPTH),
Osteoblasts (OBs),Osteocytes (OCYs), Parathyroid hormone (PTH), Primary Hyperparathyroidism (PHPT), PTH/PTHrP receptor (PPR), Stromal Cells (SCs), Tumor necrosis factor α (TNF).

SUMMARY

Primary hyperparathyroidism (PHPT) is a common cause of bone loss that is modeled in animals by continuous PTH (cPTH) infusion. Here we show that the inflammatory cytokine IL- 17A is upregulated by PHPT in humans and cPTH treatment in mice. In humans IL-17A is normalized by parathyroidectomy. In mice treatment with anti-IL-17A antibody and silencing of IL-17A receptor IL-17RA prevent cPTH induced osteocytic and osteoblastic RANKL production and bone loss. Mechanistically, cPTH stimulates conventional T cell production of TNFα (TNF), which increases the differentiation of IL-17A producing Th17 cells via TNF receptor 1 (TNFR1) signaling in CD4+ cells. Moreover, cPTH enhances the sensitivity of naïve CD4+ cells to TNF via GαS/cAMP/Ca++ signaling. Accordingly, conditional deletion of GαS in CD4+ cells and in vivo treatment with the calcium channel blocker diltiazem prevents Th17 cell expansion and blocks cPTH induced bone loss. Neutralization of IL-17A and calcium channel blockers may thus represent novel therapeutic strategies for hyperparathyroidism.

INTRODUCTION

Parathyroid hormone (PTH) is a major regulator of calcium metabolism and bone homeostasis. PHPT, a condition characterized by chronic overproduction of PTH, is a cause of increased bone turnover 1 and osteoporosis (1-3), an independent risk factor for fractures. PHPT is modeled in animals by continuous PTH (cPTH) infusion. Both PHPT and cPTH treatment stimulate bone resorption and, to a lesser extent, bone formation 4 causing cortical bone loss and often trabecular bone loss (2,5).

The effects of cPTH on bone result from its binding to the PTH/PTH-related protein (PTHrP) receptor (PPR or PTHR1), which is expressed on bone marrow (BM) stromal cells, osteoblasts and osteocytes (6,7), but also T cells (8) and macrophages (9). Early consensus held that the catabolic effect of cPTH is mediated by altered production of RANKL and OPG by stromal cells and osteoblasts (10). Osteocytes have now emerged as essential targets of PTH, as osteocyte produced RANKL is pivotal for cPTH induced bone loss (7,11,12). cPTH fails to induce bone loss in T cell null mice and mice with conditional deletion of PPR in T cells (13,14), thus revealing that Tcells contribute to the mechanism of action of PTH in bone. PPR activation in T cells stimulates TNF production by BM conventional CD4+ and CD8+ cells (14) and cPTH fails to induce bone loss in mice specifically lacking TNF production by T cells (14). TNF upregulates CD40 expression in SCs, allowing T cell expressed CD40L to regulate the responsiveness of SCs to cPTH (13).

However, TNF is likely to contribute to the bone catabolic activity of cPTH via additional effects. The mechanisms by which cPTH regulates T cell function, the specific population of T cells that mediate the activity of cPTH, and the role of T cells in the activity of PTH in humans remain to be determined.

cPTH stimulates bone and immune cells to release growth factors and cytokines. Among them are TGFβ, IL-6, and TNF (14-16), factors that direct

the differentiation of naïve CD4+ cells into Th17 cells (17-20). Th17 cells are an osteoclastogenic population of CD4+ cells (21,22) defined by the capacity to produce IL-17A and other minor members of the IL-17 family of cytokines (18). Th17 cells reside in the BM (23) and play a pathogenic role in inflammatory conditions such as psoriasis, rheumatoid arthritis, multiple sclerosis and Crohn's disease (22,24).

Moreover, Th17 cells contribute to the bone wasting caused by estrogen deficiency in mice (25,26) and humans (27,28).

Th17 cells potently induce osteoclastogenesis by secreting IL-17A, RANKL, TNF, IL-1 and IL- 6, along with low levels of IFNγ (29-31). IL-17A stimulates the release of RANKL by all osteoblastic cells including osteocytes (21,29,32) and potentiates the osteoclastogenic activity of RANKL by upregulating RANK (33). Therefore, it is plausible that cPTH may induce Th17 cell differentiation in the BM, and that IL-17A produced by BM Th17 cells may act as an upstream cytokine that plays a pivotal role in the bone loss induced by cPTH and PHPT.

This study was designed to determine the effects of PHPT and cPTH on the production of IL- 17A in humans and mice and to investigate the contribution of IL-17A to the bone loss induced by cPTH in mice. We report that PHPT increases peripheral blood cell expression of IL-17A mRNA, which is normalized by parathyroidectomy. We also show that in mice, cPTH promotes Th17 cell differentiation via TNFR1 signaling in T cells. Moreover, cPTH enhances the sensitivity of naïve CD4+ cells to TNF via the GαS/cAMP/Ca++ signaling pathway. Attesting to relevance of IL-17A and PTH signaling in T cells, silencing of IL-17RA or GαS and treatment with neutralizing anti IL-17A antibody or the calcium channel blocker diltiazem prevent cPTH induced bone loss.

RESULTS

Increased production of IL-17A in humans affected by PHPT

To investigate the effects of PHPT in the production of cytokines unfractionated peripheral blood nucleated cells were obtained from 57 healthy controls and 20 subjects affected by PHPT of similar gender, age and years since menopause. The demographic characteristics of the study population and the serum levels of calcium, phosphorous, PTH and 25-hydroxy Vitamin D are shown in table 1. In PHPT patient's blood samples were obtained before surgery and 1 month after successful resolution of PHPT by parathyroidectomy. Analysis by real time RT-PCR revealed that the mRNA levels of IL-17A in unfractionated peripheral blood nucleated cells were ~ 3 fold higher in PHPT patients than in healthy controls (fig. 1a). Moreover, surgical restoration of normal parathyroid function was associated with the normalization of IL-17A levels, as demonstrated by the finding at 1 month after parathyroidectomy of similar IL-17A mRNA levels in healthy subjects and former PHPT patients. Moreover, the mRNA levels of the IL-17-inducing transcription factor RORC were~ 3 fold higher in PHPT patients before surgery than in healthy controls (fig. 1b) and parathyroidectomy was followed by a decrease in RORC mRNA levels. As a result, levels of RORC mRNA in healthy controls and PHPT patients after surgery were not significantly different.

In the entire study population PTH levels were directly correlated with IL-17A ($r=0.38$, $p<0.005$) and RORC ($r=0.27$, $p<0.05$) mRNA levels. Moreover, disease status (healthy or PHPT) and age were independent predictors of IL-17A and RORC mRNA levels, whereas gender was not (supplementary tables 1,2). These differences in IL-17A and RORC levels between healthy controls and PHPT patients remained significant even after adjustment for age and gender by a multiple regression model.6

PHPT was also associated with increased mRNA levels of TNF and IL-23, which were normalized by parathyroidectomy. By contrast all groups had similar mRNA levels of IFNγ and IL-4 (Supplemental figure 1).

Treatment with cPTH expands Th17 cells and IL-17A production in the mouse

To investigate the effect of PTH in mice, human PTH 1-34 was continuously infused at the rate of 80 μg/kg/day for 2 weeks, a treatment modality referred to hereafter as cPTH. Analysis by flow cytometry of unfractionated peripheral blood nucleated cells harvested at sacrifice revealed that cPTH increased the relative and absolute frequency of peripheral blood Th17+ cells (fig. 2a-c). Moreover, cPTH increased IL-17A mRNA levels in purified peripheral blood CD4+ cells (fig. 2d) and unfractionated peripheral blood nucleated cells, but not in CD4+ cell depleted peripheral blood nucleated cells (fig.2e), indicating that CD4+ cells represent the major source of IL-17 mRNA in peripheral blood cells.

Mirroring its activity in peripheral blood, cPTH increased by ~2 fold the relative and absolute frequency of Th17 cells in the BM (fig. 2f,g), by ~5 fold the levels of IL-17A mRNA in purified BM CD4+ cells (fig. 2h), and by 2 fold the levels of IL-17A protein in the culture media of BM CD4+ cells (fig. 2i). Moreover, cPTH increased the expression of the Th17-inducing transcription factors RORα and RORγt in BM CD4+ T cells (fig. 2j). cPTH treatment was also associated with a ~2 fold increase in the relative and absolute frequency of splenic Th17 cells (fig. 2k,l) and a ~4 fold increase in the levels of IL-17A mRNA in purified splenic CD4+ cells (fig. 2m). By contrast, cPTH did not increase the relative and absolute frequency of IFNγ+CD4+ cells, IL-4+CD4+ cells, and FoxP3+CD4+ cells in the peripheral blood, BM and spleen (Supplemental figure 2),

indicating that cPTH does not expand murine Th1 cells, Th2 cells and regulatory T cells.7

cPTH fails to induce bone loss in WT mice treated with anti IL-17A antibody and in IL- 17RA-/- mice

To investigate whether IL-17A contributes to the bone catabolic activity of cPTH, WT mice were treated with vehicle or cPTH and either a neutralizing antibody directed against murine IL- 17A (IL-17A Ab) or isotype matched irrelevant Ab (Irr.Ig), at the dose of 2.5 mg/kg, twice per week for 2 weeks. To assess the differential effects of cPTH on cortical and trabecular bone, micro-computed tomography (μCT) was utilized to analyze femurs harvested at sacrifice. cPTH induced significant loss of cortical thickness (Ct.Th) and volume (Ct.Vo) and trabecular bone volume (BV/TV) in mice treated with Irr.Ig, but not in those treated with IL-17A Ab (fig.3a).

Analysis of indices of trabecular structure revealed that cPTH had opposite effects in trabecular number (Tb.N) in mice treated with Irr.Ig and those treated with IL-17A Ab. A similar trend was observed for trabecular space (Tb.Sp). By contrast, cPTH induced decreased trabecular thickness (Tb.Th) in all mice (Supplemental figure 3).

Analysis of femoral cancellous bone by histomorphometry revealed that cPTH treatment increased two indices of bone resorption, the number of OCs per bone surface (N.Oc/BS) and the percentage of surfaces covered by OCs (Oc.S/BS), in mice treated with Irr. Ab but not in those treated with IL-17Ab (fig.3b). Analysis of dynamic indices of bone formation revealed that cPTH increased mineral apposition rate (MAR) and bone formation rate (BFR) in mice treated with Irr. Ab and in those treated with IL-17A Ab (fig.3c). Two static indices of bone formation, the number of OBs per bone surface (N.Ob/BS) and the percentage of surfaces covered by OBs (Ob.S/BS) increased significantly in response to treatment with cPTH in both mice

treated with Irr. Ig and those treated with IL-17A Ab (fig.3c). These indices were unexpectedly higher in the vehicle/IL-17A Ab group as compared to the vehicle/Irr. Ab group. These findings indicate that neutralization of IL-17A blunts the bone catabolic activity of cPTH by decreasing bone resorption. Confirmation was provided by measurements of serum levels of C-terminal 8 telopeptide of collagen (CTX), a marker of bone resorption, and total procollagen type 1 Nterminal propeptide (P1NP), a marker of bone formation. These assays revealed that treatment with IL-17A Ab significantly blunted the increase in serum CTX levels induced by cPTH, while it did not diminish the cPTH induced increase in P1NP levels (fig.3d). Together, the data demonstrate neutralization of IL-17A blunts the capacity of cPTH to stimulate bone resorption without affecting bone formation. These changes in bone turnover prevented bone loss but did not cause a significant increase in bone volume presumably because of the short duration of the IL-17Ab treatment. Osteocyte-produced RANKL is now known to be critical for cPTH induced bone loss 7,11,12. IL- 17A Ab completely blocked the increase in osteocytic RANKL mRNA levels induced by cPTH (fig.3e), indicating that IL-17A may mediate the bone catabolic activity of cPTH by upregulating the production of RANKL by osteocytes. Further attesting to causal role of IL-17A, we found that treatment with IL-17A Ab completely blocked the capacity of cPTH treatment to increase the expression of RANKL, TNF, IL-1β and IL-6 mRNAs in purified osteoblasts and the increase in the expression of TNF mRNA in purified BM T cells (Supplemental figure 4a).

IL-17A binds to the heterodimeric receptor IL-17RA/IL-17RC known as IL-17RA 34,35. IL-17A signaling is silenced in IL-17RA-/- mice 36. We made use of IL-17RA-/- mice to further investigate whether IL-17A contributes to the bone catabolic activity of cPTH. 16 week-old IL- 17RA-/- mice and WT littermates were treated with vehicle or cPTH for 2 weeks. In vitro μCT analysis of femurs harvested at sacrifice revealed that cPTH induced

significant losses of Ct.Th, Ct.Vo and BV/TV in WT mice but not in IL-17RA-/- mice (fig.3f). For reasons that remain undetermined, Ct.Th was lower in vehicle treated IL-17RA-/- mice as compared to vehicle treated WT mice. Parameters of trabecular structure (Tb.N, Tb.Th, and Tb.Sp) were altered by cPTH in WT but not in IL-17RA-/- mice (Supplemental figure 5).
Serum CTX levels were increased by cPTH in WT but not in IL-17RA-/- mice (fig.3g). By contrast serum P1NP levels were increased by cPTH in WT and IL-17RA-/- mice (fig.3g). Osteocytic RANKL mRNA levels were increased by cPTH in WT but not in IL-17RA-/- mice (fig.3h). Finally, cPTH treatment increased the osteoblastic expression of RANKL, TNF, IL-1β and IL-6 mRNAs and the T cell expression of TNF mRNA in in WT but not IL-17RA-/- mice (Supplemental figure 4b). These findings demonstrate that silencing of IL-17RA prevents the loss of cortical and trabecular bone, and the increase in bone resorption and the osteoblastic/osteocytic RANKL production induced by cPTH.

cPTH increases the differentiation of Th17 cells via a TNF dependent mechanism

We utilized BM cells, which are essential for the regulation of bone homeostasis, and cells from the spleen, an organ not known to regulate bone remodeling to determine the mechanism by which cPTH expands Th17 cells. BrdU incorporation studies revealed that cPTH did not increase the proliferation of Th17 cells in the BM and the spleen (Supplemental figure 6a,b). IL- 17A-eGFP mice were utilized to investigate the differentiation of naïve CD4+ cells into Th17 cells. IL-17A-eGFP reporter mice possess an IRES-eGFP sequence after the stop codon of the IL17A gene so that eGFP expression is limited to IL-17A expressing cells, allowing Th17 cells to be detected by measuring eGFP by flow cytometry. Splenic naïve CD4+ cells (CD4+CD44loCD62LhieGFP- cells) were FACS sorted from IL-17A-eGFP

mice and transferred into congenic T cell deficient TCRβ-/- mice. Recipient mice were treated with vehicle or cPTH for 2 weeks starting 2 weeks after the T cell transfer, and newly produced Th17 cells (CD4+eGFP+ cells) counted. Since TCRβ-/- mice were reconstituted with eGFP- cells, the number of eGFP+ cells in host mice at sacrifice provides a direct quantification of the differentiation of naïve CD4+ cells into Th17 cells. cPTH treated mice had a higher number (10) eGFP+ cells than controls in the BM and the spleen (Supplemental figure 6c,d) demonstrating that cPTH increases Th17 cell differentiation in the BM and the spleen. TNF expands Th17 cells and mediates the catabolic activity of cPTH 19,20,37. Therefore, we investigated the overall contribution of TNF and the specific role of T cell produced TNF in the expansion of Th17 cells induced by cPTH. WT and TNF-/- mice were treated with cPTH for 2 weeks and the relative frequency of BM Th17 cells determined. cPTH increased the frequency of Th17 cells in the spleen and the BM in WT mice, but not in TNF-/- mice (fig. 4a,b). Analysis of purified BM CD4+ cells revealed that cPTH increased IL-17A mRNA levels (fig. 4c) and the expression of RORα and RORγt (fig. 4d,e) in BM CD4+ cells from WT but not in those from TNF-/- mice. Thus, cPTH induces Th17 cells via TNF. Next, splenic T cells from WT and TNF-/-mice were transferred into TCRβ-/- mice. Recipient mice were treated with vehicle or cPTH for 2 weeks starting 2 weeks after the T cell transfer. cPTH increased the number of Th17 cells (fig.4f), IL-17A mRNA levels in CD4+ cells (fig. 4g) and the expression of RORα and RORγt in
CD4+ cells (fig. 4h,i) in the BM of host mice with WT T cells but not in those with TNF-/- T cells. These findings demonstrate that the production of TNF by T cells is required for cPTH to expand Th17 cells.

To determine whether TNF directly targets Th17 precursors, splenic CD4+ cells from TNFR1-/- and TNFR2-/- mice were transferred into TCRβ-/- mice. Host mice were treated with vehicle or cPTH for 2 weeks starting 2 weeks

after the T cell transfer. cPTH expanded BM Th17 cells in mice with TNFR2-/- T cells but not in those with TNFR1-/- T cells (fig. 4f). Moreover, cPTH increased IL-17A mRNA levels in BM CD4+ cells (fig. 4g) and the BM CD4+ cell expression of RORα and RORγt (fig. 4h,i) in mice with TNFR2-/- T cells but not in those with TNFR1-/- T cells.

These findings demonstrate that cPTH expands the pool of BM Th17 cells through direct TNFR1 signaling in T cells. 11

In addition to TNF, several cytokines are known to promote Th17 cell expansion. Among them are the T cell produced factor IL-21 and the macrophage/dendritic cell produced cytokine IL-23. We found that cPTH treatment increased the mRNA levels of IL-21, and IL-23R in BM and spleen CD4+ cells from WT but not TNF-/- mice (Supplemental figure 7a,b). Moreover, cPTH increased the mRNA levels of IL-23 in BM CD11c+ cells from WT but not TNF-/- mice (Supplemental figure 7c). These findings suggest that IL-21 and IL-23 may contribute to expansion of Th17 cells induced by cPTH. However, cPTH upregulates these factors via TNF.

cPTH increases the sensitivity of nascent Th17 cells to TNF via GαS signaling

Conditional deletion of the G protein-coupled receptor subunit GαS in T cells impairs the generation of Th17 cells 38. Since PTH binding to PPR activates GαS 39, cPTH could further upregulate Th17 differentiation by activating GαS in naïve CD4+ T cells. To investigate the role of GαS we generated GαSΔCD4,8 mice by crossing C57BL6 GαS fl/fl mice with C57BL6 CD4-Cre mice, as previously described by Li et al 38. The targeted genetic deletion of GαS with CD4-Cre occurs at the CD4+CD8+ double positive stage of T cell development 38. Consequently both CD4+ and CD8+ T cells from GαSΔCD4,8 mice lack GαS expression. GαSΔCD4,8, Gαs fl/fl, and WT mice have similar numbers of CD4+ and CD8+ cells, and similar percentages of

effector, memory, and naïve CD4+ and CD8+ cells 38. One mechanism by which activation of GαS in CD4+ cells could promote Th17 cell differentiation is increased sensitivity to TNF. To investigate this hypothesis, naïve splenic CD4+ cells from vehicle and cPTH treated WT, GαS fl/fl and GαSΔCD4,8 mice were cultured *in vitro* in anti-CD3 Ab and anti-CD28 coated wells for 3 days in the presence of TNF at 10-50 ng/ml to induce the conversion of CD4+cells into Th17 cells. Cultures of CD4+ cells from cPTH treated WT and GαS fl/fl mice yielded a higher number of Th17 cells as compared to those from vehicle 12 treated mice (fig.5a). By contrast cultures of CD4+ cells from vehicle and cPTH treated GαSΔCD4,8 mice yielded similar numbers of Th17 cells, demonstrating that cPTH increases the sensitivity of nascent Th17 cells to TNF via GαS signaling in CD4+ cells. Mechanistic studies revealed that treatment with cPTH for 2 weeks increased the mRNA levels of TNFR1 and the TNFR1 activated signaling molecule TRAF240 in BM CD4+ cells from of WT and Gαs fl/fl mice but not in those from GαSΔCD4,8 mice (fig.5b,c) indicating that activation of GαS signaling by cPTH increases the sensitivity of nascent Th17 cells to TNF by upregulating TNFR1 expression and TNFR1 signaling.

Treatment of GαSΔCD4,8 and Gαs fl/fl control mice with cPTH for 2 weeks increased the frequency of BM Th17 cells (fig.5d), and induced significant losses of Ct.Th, Ct.Vo, and BV/TV (fig.5e-g), and Tb.Th (Supplemental figure 8a) in GαS fl/fl mice but not GαSΔCD4,8 mice. Unexpectedly, cPTH did not affect Tb.Sp and Tb.N in all mice (Supplemental figure 8b,c). cPTH also increased serum CTX levels in GαS fl/fl but not GαSΔCD4,8 mice (fig. 5h). Serum P1NP and osteocalcin (OCN) levels were increased by cPTH in GαS fl/fl and GαSΔCD4,8 mice (fig. 5i,j).

These findings demonstrate that silencing of Gαs in T cells prevents the expansion of Th17 cells, the loss of cortical and trabecular bone, and the increase in bone resorption induced by cPTH.

Signaling events downstream of GαS include cAMP generation 38 and activation of L-type calcium channels 41. The latter contributes to Th17 cell differentiation 42. Accordingly, in vitro treatment with the L-type calcium channel blocker diltiazem blunts the differentiation of CD4+ cells into Th17 cells 38. We fed mice with or without diltiazem in their drinking water, as described 43,44 and infused them with vehicle or cPTH. Diltiazem blocked the increase in the number of BM Th17 cells (fig.6a), the BM mRNA levels of IL-17A (fig.6b), and the BM CD4+ cell expression of RORα and RORγt (fig.6c,d) induced by cPTH. Moreover, diltiazem completely blocked the decrease in Ct.Vo, Ct.Th and BV/TV induced by cPTH (fig.6e-g) and altered the 13 response to cPTH of parameters of trabecular structure (fig.6h-j). Diltiazem blocked the increase in serum CTX levels but not the increase in serum P1NP induced by cPTH (fig.6k,l). These findings demonstrate that diltiazem prevents the loss of cortical and trabecular bone induced by cPTH by blunting bone resorption.

DISCUSSION

We report that in humans the levels of IL-17A mRNA in peripheral blood nucleated cells is increased by PHPT and normalized by parathyroidectomy. In mice, cPTH increases production of IL-17A and expands Th17 cells. Silencing of IL-17RA or treatment with IL-17A Ab blocks the bone loss induced by cPTH, demonstrating that IL-17A plays a pivotal role in the bone catabolic activity of cPTH. Overproduction of IL-17A has been documented in inflammatory conditions associated with local and systemic bone loss such as psoriasis, rheumatoid arthritis and Crohn's disease (22,24). To the best of our knowledge this is the first study to demonstrate that patients affected by PHPT have increased expression of IL-17A and RORC genes that are normalized by parathyroidectomy. IL-17A levels are affected by age and

gender (45,46). However the association between increased IL-17A and RORC mRNA levels persisted when the effects of age and gender were adjusted for in a multivariable analysis. Our findings suggest that increased IL-17A gene expression in PHPT patients is due to increased levels of circulating PTH but we cannot exclude that IL-17A might be regulated by factors modified by PTH, such as serum levels of calcium, phosphate and calcitriol. A previous cross-sectional study in patients on dialysis with hyperparathyroidism secondary to end-stage renal disease revealed a direct correlation between phosphate levels and frequency of peripheral blood Th17 cells (47). By contrast, in our study IL-17A levels were increased in PHPT patients who have decreased phosphate levels. Moreover, we found no correlation between IL-17A and RORC expression and serum phosphate levels. Further studies will be required to determine if phosphate regulates Th17 cells in healthy subjects and patients with primary and secondary hyperparathyroidism. Whether PHPT increases levels of IL-17A protein in the peripheral circulation and in the BM remains to be determined. However, the findings in a mouse model of PHPT reported herein, including the capacity of IL-17A and IL-17RA neutralization to prevent cPTH induced bone loss, suggest that IL-17A plays a pivotal role in the bone disease caused by PHPT. IL-6 and TGFβ initiate Th17 differentiation (18,24) while TNF, IL-1, and IL-23 amplify it (48). The relevance of TNF for Th17 cell expansion has emerged by investigations on the effects of TNF blockers, which have demonstrated that TNF contributes to the expansion of Th17 cells in inflammatory conditions in humans and rodents (19,20). Accumulation of cAMP in CD4+ cells and the resulting Ca2+ influx further promote Th17 cell differentiation and activity 38. Treatment with cPTH induces the production of IL-6 and TGFβ by bone and immune cells (15,16) and the release of TNF by BM CD4+ and CD8+ cells (14). PTH binding to PPR activates the G protein-coupled receptor subunit GαS, leading to the generation of cAMP (39). Therefore, several mechanisms

could account for the capacity of cPTH to expand Th17 cells. We found T cell produced TNF and activation of TNFR1 signaling in CD4+ cells to be required for cPTH to expand murine Th17 cells. Human and murine data indicate that TNF acts directly and by upregulating the Th17 inducing factors IL-21 and IL-23. However, our findings do no exclude the possibility that PTH mediated stimulation of IL-6 and TGFβ production may contribute to the expansion of Th17 cells induced by cPTH. Moreover, cPTH increases the sensitivity of naïve CD4+ cells to TNF by upregulating TNFR1 and the signaling molecule TRAF2 (40), via activation of the GαS/cAMP pathway in CD4+ cells and the resulting increase in L-type calcium channel-mediated Ca2+ influx. The finding that *in vivo* treatment with diltiazem blocks Th17 cell expansion and prevents cPTH induced bone loss may suggest a potential therapeutic role for L-type calcium channel blockers in the treatment of hyperparathyroidism, even though the available data do not exclude the possibility of additional effects of diltiazem on immune cells that may contribute to its bone sparing activity. The pool of RANKL produced by osteocytes is crucial for the activity of cPTH. In fact, not only does silencing of PPR expression in osteocytes results in higher baseline bone volume and (16) blunts the bone catabolic activity of cPTH (7), but increased production of RANKL by osteocytes is now known to play a pivotal role in cPTH induced bone loss (7,11,12). Earlier reports had disclosed that IL-17A is a potent inducer of RANKL in organ cultures containing osteoblasts and osteocytes (49). In the current study we have found that neutralization of IL-17A and silencing of IL-17RA block the capacity of cPTH to increase the production of RANKL by osteocytes. We also found IL-17A and IL-17RA signaling to be required for cPTH to stimulate osteoblastic RANKL. These findings indicate that IL-17A acts as an upstream cytokine that drives bone loss by upregulating the production of osteocytic and osteoblastic RANKL. Therefore T cells, osteoblasts and osteocytes are all key targets of cPTH, as the presence of T cell derived signals that

increase the sensitivity of osteoblastic cells to cPTH is required for the hormone to exert its full bone catabolic activity. However, since mice lacking IL-17RA signaling and those lacking PPR signaling in T cells (14,50) do not have an increased baseline bone volume, the data suggest that neither PPR signaling in T cells nor IL-17A signaling are required for physiologic levels of endogenous PTH to regulate bone remodeling.

Although IL-17A is mostly produced by Th17 cells derived from CD4+ cells, $\gamma\delta$ T cells, innate lymphoid cells, NK cells, NKT cells, neutrophils and eosinophils have also been shown to produce IL-17 (51-53). Our data do not support a role for $\gamma\delta$ T cell produced IL-17A in the bone catabolic activity of cPTH because TCRβ-/- mice, a strain lacking $\alpha\beta$ but not $\gamma\delta$ T cells are completely protected against cPTH induced bone loss (13).

The bone catabolic activity of cPTH is due to a stimulation of bone resorption mitigated by a concomitant increase in bone formation. Analysis of histomorphometric and biochemical indices of bone turnover revealed that neutralization of IL-17A and IL-17RA blunts the stimulation of bone resorption induced by cPTH. The blockade of bone resorption induced by IL-17 Ab was of greater magnitude when estimated by serum levels of CTX than when measured by bone histomorphometry. The likely explanation for this phenomenon is that CTX levels reflect both (17) cortical and trabecular bone resorption while histomorphometric indices were calculated only in the trabecular compartment. This is relevant because cortical bone accounts for most of the total bone mass and cPTH affects primarily the cortical compartment of the skeleton. Direct clinical applications of these findings arise because anti human IL-17A Abs and IL-17 receptor Abs are under investigation as therapeutic agents in psoriasis and spondyloarthropathy (54-57). Therefore our findings demonstrate a novel role for IL-17A in the mechanism of action of cPTH and provide a proof of principle for the use of IL-17A Ab in the treatment of primary hyperparathyroidism. (18)

AUTHOR CONTRIBUTIONS: PDA, FS, IB and GCI designed the human studies, performed the human research, and analyzed the human data. RP, JYL and MNW designed the animal study/protocols. JYL, JR, LDW, CV, TL, AMT, MY, MR, and JA performed the animal research and analyzed the data. RP wrote the manuscript and was the principle investigator.

ACKNOWLEDGEMENTS

We are grateful to Prof. L. Richiardi (University of Turin, Italy) for his assistance with the statistical analysis of the human data, Dr. Weinstein (NIH) for providing the Gαs fl/fl mice and to Amgen, Inc for providing the IL-17RA-/- mice. This study was supported by grants from the National Institutes of Health (AR54625, DK007298 and RR028009). JYL was supported by a grant from the National Institutes of Health (AR061453). MNW was supported in part, by a grant from the Biomedical Laboratory Research & Development Service of the VA Office of Research and Development (5I01BX000105) and by NIH grants R01AR059364 and R01AG040013.

DISCLOSURES

The authors state that they have no conflicts of interest.

EXPERIMENTAL PROCEDURES

Study design. See supplemental experimental procedures.

Human Study population. All human studies were approved by the Ethical Committee of theA.O.U. Città della Salute e della Scienza - A.O. Ordine Mauriziano - A.S.L. TO1, Turin Italy and informed consent was obtained from all participants. The study population was recruited from the patients of A.O.U. Città della Salute e della Scienza, Turin Italy and healthy volunteers. The study population included 20 patients (16 women and 4 men) affected by primary hyperparathyroidism (PHPT) and 57 healthy subjects (25 males and 32 females) comparable for age and years since menopause. The demographic characteristics of the study population are shown in table 1. The diagnosis of PHPT was established based on the finding of elevated circulating levels of calcium and PTH in at least 2 instances and the presence of normal renal function. PHPT patients were subjected to parathyroidectomy and restoration of normal parathyroid function was demonstrated by the finding of normal serum PTH levels 1 month after surgery. Inclusion and exclusion criteria are provided in supplemental experimental procedures.

Measurements of IL-17A, TNFα, IL-23, IL-4, IFNγ and RORC mRNAs in human samples.

See supplemental experimental procedures.

Animals. All the animal procedures were approved by the Institutional Animal Care and Use Committee of Emory University. Additional information is provided in supplemental experimental procedures.

In vivo cPTH treatment. 80 µg/kg/day of hPTH1-34 (Bachem California Inc., Torrance, CA) or vehicle were infused for 2 weeks in 16 weeks old female mice by implanting ALZET osmotic pump model-1002 (DURECT corporation Cupertino, CA) with a delivery rate of 0.24 ml/hr, as previously described 13,14. 20

IL-17A Ab treatment. 16 week-old WT mice were infused with vehicle or PTH for 2 weeks. These mice were also injected with mouse IL-17A neutralizing antibody (IL-17A Ab) (R&D Systems, MAB421) or isotype matched irrelevant Ab (Irr.Ig) at 2.5 mg/kg, twice per week.

Diltiazem treatment. 16 week-old WT mice were infused with vehicle or PTH for 2 weeks. These mice received regular water or 100mg/kg body weight/day Diltiazem (Enzo life Science, Inc. Farmingdale, NY) with the drinking water. **T cell transfers.** See supplemental experimental procedures.

BrdU incorporation. See supplemental experimental procedures.

In vivo and in vitro Th17 cell differentiation and IL-17A ELISA. See supplemental experimental procedures.

μCT measurements. μCT scanning and analysis was performed as reported previously (8,14) using a Scanco μCT-40 scanner. Additional information in supplemental experimental procedures.

Quantitative bone histomorphometry. The measurements, terminology and units used for histomorphometric analysis, were those recommended by the Nomenclature Committee of the American Society of Bone and Mineral Research 58. Additional information is provided in supplemental experimental procedures.

Osteoblast purification. BM cells were collected at sacrifice and OBs were purified as previously described 13,50. Additional information is provided in supplemental experimental procedures.

RNA isolation from enriched osteocytes. See supplemental experimental procedures.

Markers of bone turnover. See supplemental experimental procedures.

Flow cytometry and cell sorting. See supplemental experimental procedures.

Real-time RT-PCR and murine primers. The expression levels of murine IL-17A, I RORα,

RORγt, IL-21, IL-23, IL-23R, TNFR1, TRAF2, IL-1β, IL-6, RANKL and

TNFα mRNAs levels were 21 quantified by real-time RT-PCR. Additional information is provided in supplemental experimental procedures.

Statistical Analysis. See supplemental experimental procedures. 22

REFERENCES

1. Parisien, M., Dempster, D.W., Shane, E. & Bilezikian, J.P. Histomorphometric analysis of bone in primary hyperparathyroidism. in *The parathyroids. Basic and clinical concepts* 423-436 (Academic Press, San Diego, 2001).

2. Potts, J. Primary hyperparathyroidism. in *Metabolic Bone Diseases*, Vol. 1 (eds. Avioli, L.V. & Krane, S.) 411-442 (Academic Press, San Diego, 1998).

3. Silverberg, S.J.*, et al.* Skeletal disease in primary hyperparathyroidism. *J Bone Miner Res* **4**, 283-291 (1989).

4. Qin, L., Raggatt, L.J. & Partridge, N.C. Parathyroid hormone: a double-edged sword for bone metabolism. *Trends Endocrinol Metab* **15**, 60-65 (2004).

5. Iida-Klein, A.*, et al.* Short-term continuous infusion of human parathyroid hormone 1-34 fragment is catabolic with decreased trabecular connectivity density accompanied by hypercalcemia in C57BL/J6 mice. *J Endocrinol* **186**, 549-557 (2005).

6. Calvi, L.M.*, et al.* Activated parathyroid hormone/parathyroid hormone-related protein receptor in osteoblastic cells differentially affects cortical and trabecular bone. *J Clin Invest* **107**, 277-286 (2001).

7. Saini, V.*, et al.* Parathyroid hormone (PTH)/PTH-related peptide type 1 receptor (PPR) signaling in osteocytes regulates anabolic and catabolic skeletal responses to PTH. *The Journal of biological chemistry* **288**, 20122-20134 (2013).

8. Terauchi, M.*, et al.* T lymphocytes amplify the anabolic activity of parathyroid hormone through Wnt10b signaling. *Cell metabolism* **10**, 229-240 (2009).

9. Cho, S.W.*, et al.* Osteal macrophages support physiologic skeletal remodeling and anabolic actions of parathyroid hormone in bone. *Proc Natl Acad Sci U S A* (2014).23
10. Ma, Y.L.*, et al.* Catabolic effects of continuous human PTH (1--38) in vivo is associated with sustained stimulation of RANKL and inhibition of osteoprotegerin and gene-associated bone formation. *Endocrinology* **142**, 4047-4054 (2001).
11. Xiong, J.*, et al.* Osteocyte-derived RANKL is a critical mediator of the increased bone resorption caused by dietary calcium deficiency. *Bone* **66C**, 146-154 (2014).
12. Ben-awadh, A.N.*, et al.* Parathyroid hormone receptor signaling induces bone resorption in the adult skeleton by directly regulating the RANKL gene in osteocytes. *Endocrinology* **155**, 2797-2809 (2014).
13. Gao, Y.*, et al.* T cells potentiate PTH-induced cortical bone loss through CD40L signaling. *Cell metabolism* **8**, 132-145 (2008).
14. Tawfeek, H.*, et al.* Disruption of PTH Receptor 1 in T Cells Protects against PTH Induced Bone Loss. *PLoS ONE* **5**, e12290 (2010).
15. Lowik, C.W.G.M.*, et al.* Parathyroid hormone (PTH) and PTH-like protein (PLP) stimulate IL-6 production by osteogenic cells: a possible role of interleukin-6 in osteoclastogensis. *Biochem.Biophys.Res.Commun.* **162**, 1546-1552 (1989).
16. Koh, A.J.*, et al.* An irradiation-altered bone marrow microenvironment impacts anabolic actions of PTH. *Endocrinology* **152**, 4525-4536 (2011).
17. Bettelli, E.*, et al.* Reciprocal developmental pathways for the generation of pathogenic effector TH17 and regulatory T cells. *Nature* **441**, 235-238 (2006).
18. Basu, R., Hatton, R.D. & Weaver, C.T. The Th17 family: flexibility follows function. *Immunol Rev* **252**, 89-103 (2013).

19. Nakae, S., Suto, H., Berry, G.J. & Galli, S.J. Mast cell-derived TNF can promote Th17 cell-dependent neutrophil recruitment in ovalbumin-challenged OTII mice. *Blood* **109**, 3640-3648 (2007).
20. Sugita, S.*, et al.* Inhibition of Th17 differentiation by anti-TNF-alpha therapy in uveitis patients with Behcet's disease. *Arthritis Res Ther* **14**, R99 (2012).
21. Sato, K.*, et al.* Th17 functions as an osteoclastogenic helper T cell subset that links T cell activation and bone destruction. *J Exp Med* **203**, 2673-2682 (2006).
22. Miossec, P., Korn, T. & Kuchroo, V.K. Interleukin-17 and type 17 helper T cells. *N Engl J Med* **361**, 888-898 (2009).
23. Kappel, L.W.*, et al.* IL-17 contributes to CD4-mediated graft-versus-host disease. *Blood* **113**, 945-952 (2009).
24. Martinez, G.J., Nurieva, R.I., Yang, X.O. & Dong, C. Regulation and function of proinflammatory TH17 cells. *Ann N Y Acad Sci* **1143**, 188-211 (2008).
25. Tyagi, A.M.*, et al.* Estrogen deficiency induces the differentiation of IL-17 secreting Th17 cells: a new candidate in the pathogenesis of osteoporosis. *PLoS ONE***7**, e44552 (2012).
26. DeSelm, C.J.*, et al.* IL-17 mediates estrogen-deficient osteoporosis in an Act1-dependent manner. *Journal of cellular biochemistry* **113**, 2895-2902 (2012).
27. Molnar, I., Bohaty, I. & Somogyine-Vari, E. IL-17A-mediated sRANK ligand elevation involved in postmenopausal osteoporosis. *Osteoporos Int* **25**, 783-786 (2014).
28. Zhang, J.*, et al.* Changes of serum cytokines-related Th1/Th2/Th17 concentration in patients with postmenopausal osteoporosis. *Gynecological endocrinology : the official journal of the International Society of Gynecological*

Endocrinology, 1-8 (2014).
29. Komatsu, N. & Takayanagi, H. Autoimmune arthritis: the interface between the immune system and joints. *Advances in immunology* **115**, 45-71 (2012).
30. Waisman, A. T helper cell populations: as flexible as the skin? *European journal of immunology* **41**, 2539-2543 (2011).
31. Jovanovic, D.V.*, et al.* IL-17 stimulates the production and expression of proinflammatory cytokines, IL-beta and TNF-alpha, by human macrophages. *J Immunol* **160**, 3513-3521 (1998).
32. Kotake, S.*, et al.* IL-17 in synovial fluids from patients with rheumatoid arthritis is a potent stimulator of osteoclastogenesis. *J Clin Invest* **103**, 1345-1352 (1999).
33. Adamopoulos, I.E.*, et al.* Interleukin-17A upregulates receptor activator of NFkappaB on osteoclast precursors. *Arthritis Res Ther* **12**, R29 (2010).
34. Iwakura, Y., Ishigame, H., Saijo, S. & Nakae, S. Functional specialization of interleukin-17 family members. *Immunity* **34**, 149-162 (2011).
35. Zepp, J., Wu, L. & Li, X. IL-17 receptor signaling and T helper 17-mediated autoimmune demyelinating disease. *Trends in immunology* **32**, 232-239 (2011).
36. Ye, P.*, et al.* Requirement of interleukin 17 receptor signaling for lung CXC chemokine and granulocyte colony-stimulating factor expression, neutrophil recruitment, and host defense. *J Exp Med* **194**, 519-527 (2001).
37. Chen, D.Y.*, et al.* Increasing levels of circulating Th17 cells and interleukin-17 in rheumatoid arthritis patients with an inadequate response to anti-TNF-alpha therapy. *Arthritis Res Ther* **13**, R126 (2011).
38. Li, X.*, et al.* Divergent requirement for Galphas and cAMP in the differentiation and inflammatory profile of distinct mouse Th subsets. *J Clin Invest* **122**, 963-973 (2012).

39. Datta, N.S. & Abou-Samra, A.B. PTH and PTHrP signaling in osteoblasts. *Cell Signal* **21**, 1245-1254 (2009).
40. Qin, J.*, et al.* TNF/TNFR signal transduction pathway-mediated anti-apoptosis and anti-inflammatory effects of sodium ferulate on IL-1beta-induced rat osteoarthritis chondrocytes in vitro. *Arthritis Res Ther* **14**, R242 (2012).
41. Hell, J.W. Beta-adrenergic regulation of the L-type Ca2+ channel Ca(V)1.2 by PKA rekindles excitement. *Science signaling* **3**, pe33 (2010).
42. Oh-hora, M. Calcium signaling in the development and function of T-lineage cells. *Immunol Rev* **231**, 210-224 (2009).
43. Semsarian, C.*, et al.* The L-type calcium channel inhibitor diltiazem prevents cardiomyopathy in a mouse model. *J Clin Invest* **109**, 1013-1020 (2002).
44. Mieth, A.*, et al.* L-type calcium channel inhibitor diltiazem prevents aneurysm formation by blood pressure-independent anti-inflammatory effects. *Hypertension* **62**,1098-1104 (2013).
45. Zhou, M.*, et al.* The effect of aging on the frequency, phenotype and cytokineproduction of human blood CD4 + CXCR5 + T follicular helper cells: comparison of aged and young subjects. *Immunity & ageing : I & A* **11**, 12 (2014).
46. Tsvetkova-Vicheva, V.*, et al.* Interleukin-17 producing T cells could be a marker for patients with allergic rhinitis. *The Israel Medical Association journal : IMAJ* **16**, 358-362 (2014).
47. Lang, C.L.*, et al.* Correlation of interleukin-17-producing effector memory T cells and CD4+CD25+Foxp3 regulatory T cells with the phosphate levels in chronic hemodialysis patients. *TheScientificWorldJournal* **2014**, 593170 (2014).
48. Veldhoen, M., Hocking, R.J., Atkins, C.J., Locksley, R.M. & Stockinger, B.

TGFbeta in the context of an inflammatory cytokine milieu supports de novo differentiation of IL-17-producing T cells. *Immunity* **24**, 179-189 (2006).
49. Nakashima, T.*, et al.* Protein expression and functional difference of membranebound and soluble receptor activator of NF-kappaB ligand: modulation of the expression by osteotropic factors and cytokines. *Biochem Biophys Res Commun* **275**, 768-775 (2000).
50. Bedi, B.*, et al.* Silencing of parathyroid hormone (PTH) receptor 1 in T cells blunts the bone anabolic activity of PTH. *Proc Natl Acad Sci U S A* **109**, E725-733 (2012).
51. Korn, T., Bettelli, E., Oukka, M. & Kuchroo, V.K. IL-17 and Th17 Cells. *Annual review of immunology* **27**, 485-517 (2009).
52. Lockhart, E., Green, A.M. & Flynn, J.L. IL-17 production is dominated by gammadelta T cells rather than CD4 T cells during Mycobacterium tuberculosis infection. *J Immunol* **177**, 4662-4669 (2006).
53. Sutton, C.E.*, et al.* Interleukin-1 and IL-23 induce innate IL-17 production from gammadelta T cells, amplifying Th17 responses and autoimmunity. *Immunity* **31**, 331- 341 (2009).
54. Leonardi, C.*, et al.* Anti-interleukin-17 monoclonal antibody ixekizumab in chronic plaque psoriasis. *N Engl J Med* **366**, 1190-1199 (2012).
55. Mease, P.J.*, et al.* Brodalumab, an anti-IL17RA monoclonal antibody, in psoriatic arthritis. *N Engl J Med* **370**, 2295-2306 (2014).
56. Yeremenko, N., Paramarta, J.E. & Baeten, D. The interleukin-23/interleukin-17 immune axis as a promising new target in the treatment of spondyloarthritis. *Current opinion in rheumatology* **26**, 361-370 (2014).
57. Martin, D.A.*, et al.* A phase Ib multiple ascending dose study evaluating safety, pharmacokinetics, and early clinical response of brodalumab, a human anti-IL-17R antibody, in methotrexate-resistant rheumatoid arthritis. *Arthritis Res Ther* **15**, R164 (2013).

58. Dempster, D.W*., et al.* Standardized nomenclature, symbols, and units for bone histomorphometry: a 2012 update of the report of the ASBMR Histomorphometry Nomenclature Committee. *J Bone Miner Res* **28**, 2-17 (2013).

FIGURE LEGEND

Figure 1. Levels (Median + interquartile range) of IL-17A and RORC mRNAs in healthy controls (n = 57) and subjects with PHPT before (n = 20) and after parathyroidectomy (n = 20). Data were analyzed by Mann Whitney (healthy controls vs. PHPT before surgery and healthy controls vs. PHPT after surgery) and Wilcoxon matched pairs signed rank tests (PHPT vs. PHPT after surgery) as the data were not normally distributed according to the Shapiro-Wilk normality test.

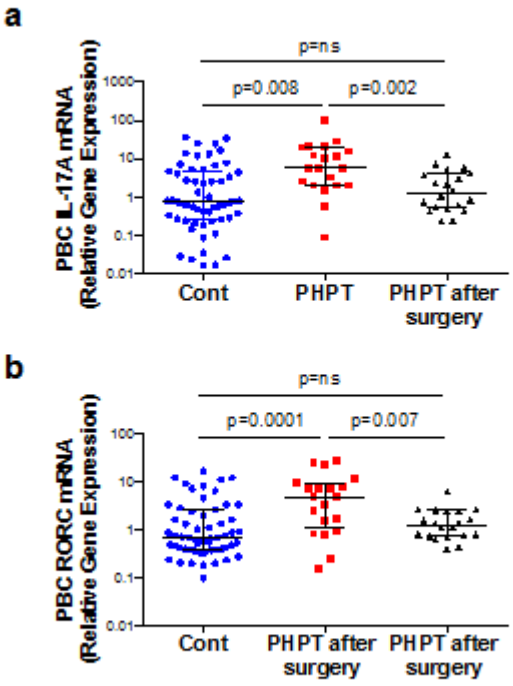

Fig 1

Figure 2. Effects of cPTH treatment on the frequency of Th17 cells and IL-17 production. **a-c.** Frequency of IL-17A producing Th17 cells in unfractionated peripheral blood (PB) cells (PBC). Panel a shows representative flow cytometric dot plots from 1 mouse per group. Panel b shows the relative frequency of CD4+IL-17A+ PBC. Data are expressed as % of CD4+ cells**.** Panel c shows the absolute number of CD4+IL-17A+ PBCs per sample**. d.** IL-17A mRNA levels in PB CD4+ cells. **e.** IL-17A mRNA levels in unfractionated PBC and CD4+ cell-depleted PBC. **f.** Relative frequency of Th17 cells in the BM. **g**. Absolute number of BM Th17 cells per sample. **h.** IL-17A mRNA levels in BM CD4+ cells. **i.** IL-17A protein levels in BM CD4+ cells. **j.** mRNA levels of the Th17 cells-inducing transcription factors RORα and RORγt in BM CD4+ cells. **k.** Relative frequency of Th17 cells in the spleen. **l.** Absolute number of Th17 cells in the spleen **m.** IL-17A mRNA levels in spleen CD4+ cells. Data in panels b-m are shown as mean + SEM. n = 8 mice per group in all panels. All data passed the Shapiro-Wilk normality test and were analyzed by unpaired t-tests **=$p<0.01$ and ***=$p<0.001$ compared to the corresponding vehicle group.

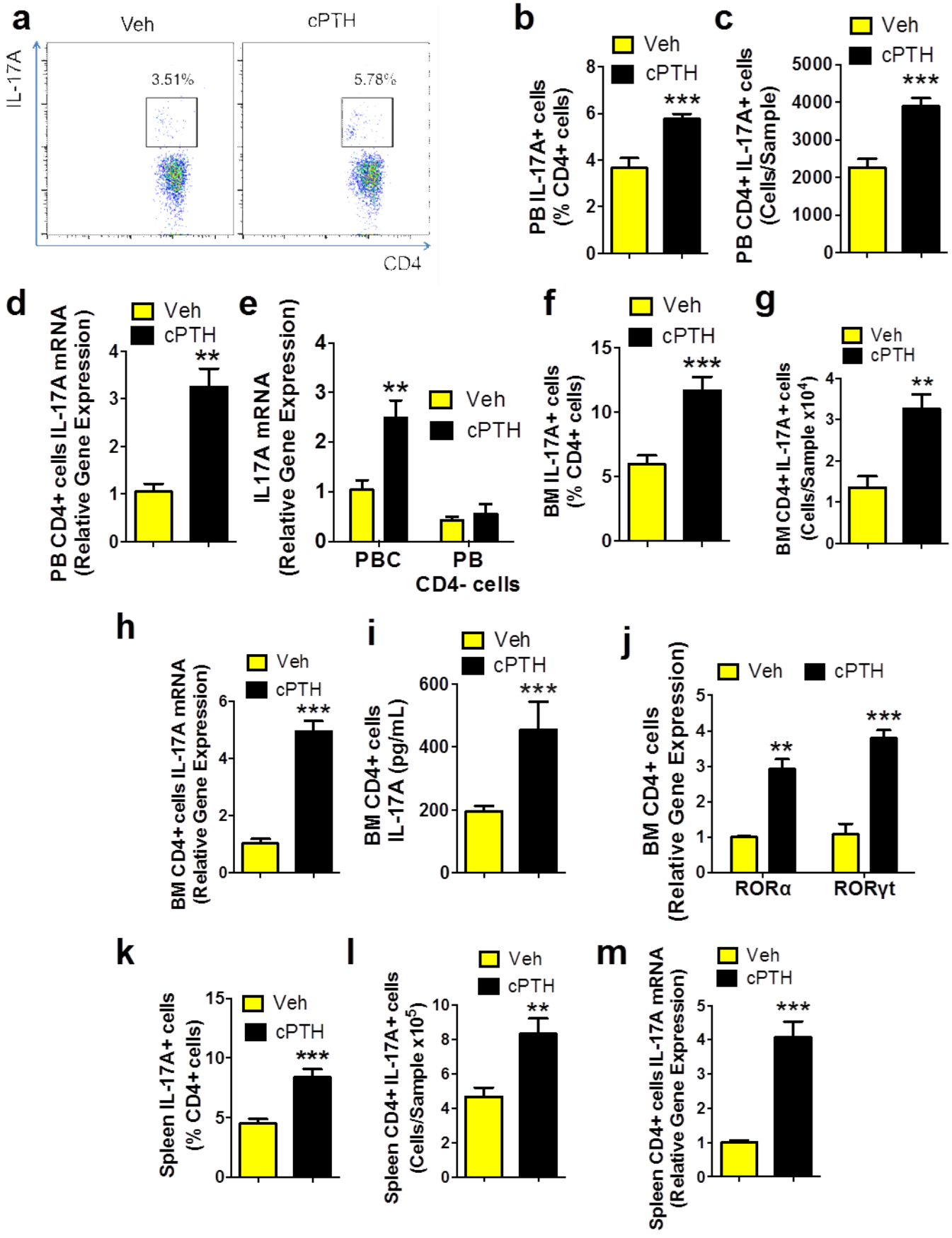
a
Veh
cPTH
IL-17A
3.51%
5.78%
CD4
b
Veh
cPTH
PB IL-17A+ cells (% CD4+ cells)
***
c
PB CD4+ IL-17A+ cells (Cells/Sample)
***
d
PB CD4+ cells IL-17A mRNA (Relative Gene Expression)
**
e
IL17A mRNA (Relative Gene Expression)
**
PBC
PB
CD4- cells
f
BM IL-17A+ cells (% CD4+ cells)
***
g
BM CD4+ IL-17A+ cells (Cells/Sample x10^4)
**
h
BM CD4+ cells IL-17A mRNA (Relative Gene Expression)
***
i
BM CD4+ cells IL-17A (pg/mL)
***
j
BM CD4+ cells (Relative Gene Expression)
**
***
RORα
RORγt
k
Spleen IL-17A+ cells (% CD4+ cells)
***
l
Spleen CD4+ IL-17A+ cells (Cells/Sample x10^5)
**
m
Spleen CD4+ cells IL-17A mRNA (Relative Gene Expression)
***

Figure 3. Effects (mean + SEM) of cPTH on bone volume, structure and turnover in mice treated with IL-17A Ab or lacking IL-1RA. **a.** In vitro measurements of cortical and trabecular bone indices of volume and structure by μCT scanning in WT mice treated with vehicle or cPTH and Irrelevant Ab (Irr. Ab) or anti IL-17A Ab. n= 12 mice per group. Representative 3- dimensional μCT reconstructions of the femurs are shown above the data. **b.** Histomorphometric indices of bone resorption (obtained in the first 10 of the 12 mice per group enrolled in the study). The images show TRAP stained sections of the distal femur used to compute the number of OCs per mm bone surface (N.Oc/BS) and the percentage of bone surface covered by OCs (Oc.S/BS),which are indices of bone resorption. Original magnification x 40. **c.** Dynamic indices of bone formation. The images show calcein double-fluorescence labeling used to compute mineral apposition rate (MAR) and bone formation rate (BFR), which are indices of bone formation. Original magnification x 20. The number of OBs per mm bone surface (N.Ob/BS) and the percentage of bone surface covered by OBs (Ob.S/BS), which are static indices of formation, were measured on trichrome-stained sections. **d**. Serum levels of CTX and P1NP. n= 12 mice per group. **e**. mRNA levels of RANKL in purified osteocytes (OCYs). n= 5 mice per group. **f**. μCT measurements of cortical and trabecular bone volume and structure in samples from WT and IL-17RA-/- mice. n = 14 mice per group. The images are 3- dimensional reconstructions of the femurs. **g**. Serum levels of CTX and P1NP. n = 14 mice per group. **h**. mRNA levels of RANKL in purified OCYs from WT and IL-17RA-/- mice. n= 5 mice per group. All data passed the Shapiro-Wilk normality test and were analyzed by 2-Way ANOVA. *= $p < 0.05$, ** = $p<0.01$ and *** = $p<0.001$ compared to the corresponding vehicle treated group. # = $p<0.05$, and ## = $p<0.01$ compared to IL-17 Ab cPTH. ###

= p<0.001 compared to IL- 17RA-/- cPTH. a= p<0.05 compared to Irr. Ab Veh. b= p<0.05 compared to WT Veh.

a

	Irr. Ab Veh	Irr. Ab cPTH	Δ	IL-17 Ab Veh	IL-17 Ab cPTH	Δ
BV/TV (%)	6.7 + 0.4	5.2 + 0.3*#	-23.1%	6.5 + 0.3	6.8 + 0.5	5.9%
Ct.Th (μm)	171.8 + 2.2	161.6 + 3.1*	-5.9%	171.8 + 1.2	170.8 + 3.2	-0.6%
Ct.Vo (mm^3)	0.67 + 0.01	0.61 + 0.01**##	-8.3%	0.66 + 0.01	0.69 + 0.01	3.6%

b

	Irr. Ab Veh	Irr. Ab cPTH	IL-17 Ab Veh	IL-17 Ab cPTH
N.Oc/BS (1/mm)	5.29 + 0.66	7.22 + 0.57*	5.31 + 0.65	6.34 + 0.46
Oc.S/BS (%)	18.91 + 2.46	26.90 + 1.81**	20.27 + 1.60	25.97 + 1.41

c

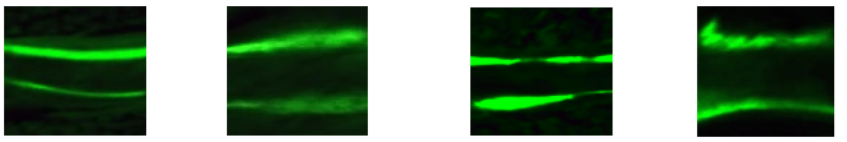

MAR (μm/day)	1.88 + 0.10	2.48 + 0.13*	1.80 + 0.13	2.71 + 0.26***
BFR (mm^3/mm^2/day)	0.45 + 0.03	0.66 + 0.05*	0.47 + 0.03	0.74 + 0.10**
N.Ob/BS (1/mm)	27.48 + 2.48	39.66 + 3.33**	39.87 + 2.77[a]	52.52 + 1.87**
Ob.S/BS (%)	38.63 + 2.22	50.23 + 3.33**	48.49 + 1.56[a]	61.72 + 1.69**

d

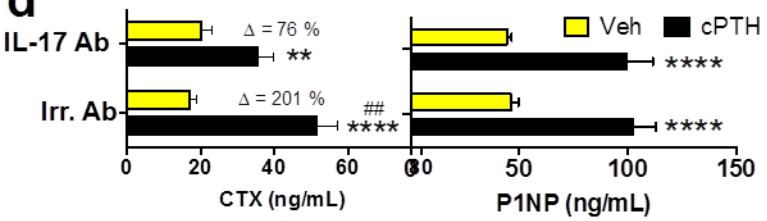

e

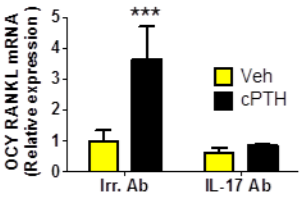

f

	WT Veh	WT cPTH	Δ	IL-17RA-/- Veh	IL-17RA-/- cPTH	Δ
BV/TV (%)	5.7 + 0.4	4.2 + 0.4*###	-25.4%	5.7 + 0.4	6.6 + 0.5	16.3%
Ct.Th (μm)	179.5 + 3.4	170.1 + 2.6*	-5.2%	166.2 + 2.6[b]	163.8 + 2.7	-1.4%
Ct.Vo (mm^3)	0.70 + 0.02	0.66 + 0.01*	-6.6%	0.66 + 0.01	0.65 + 0.01	-1.8%

g

IL-17RA KO Histo pending

h

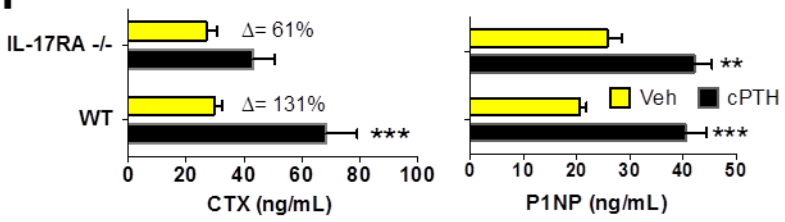

i

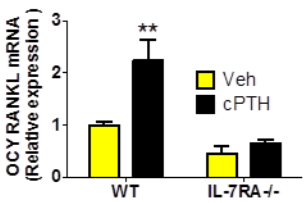

Figure 4. cPTH expands Th17 cells through TNF and TNFR1 signaling. **a-b.** Relative frequency of Th17 cells in the spleen and BM of WT and TNF-/- mice. **c.** IL-17A mRNA levels in BM CD4+ cells of WT and TNF-/- mice. **d,e.** RORα and RORγt mRNA levels in BM CD4+ cells of WT and TNF-/- mice. **f.** Relative frequency of Th17 cells in the BM of TCRβ-/- mice previously subjected to adoptive transfer of WT T cells, TNF-/- T cells, TNFR1-/- T cells, or TNFR2-/- T cells. **g.** IL-17A mRNA levels in BM CD4+ cells of TCRβ-/- mice previously subjected to adoptive transfer of WT T cells, TNF-/- T cells, TNFR1-/- T cells, or TNFR2-/- T cells. **h,i.** Levels of RORα and RORγt mRNA in BM CD4+ cells of TCRβ-/- mice previously subjected to adoptive transfer of WT T cells, TNF-/- T cells, TNFR1-/- T cells, or TNFR2-/- T cells. Data are expressed as the mean + SEM. n = 8 mice per group. All data passed the Shapiro-Wilk normality test and were analyzed by 2-Way ANOVA.*=$p<0.05$, **=$p<0.01$ and ***=$p<0.001$ compared to the corresponding vehicle group.

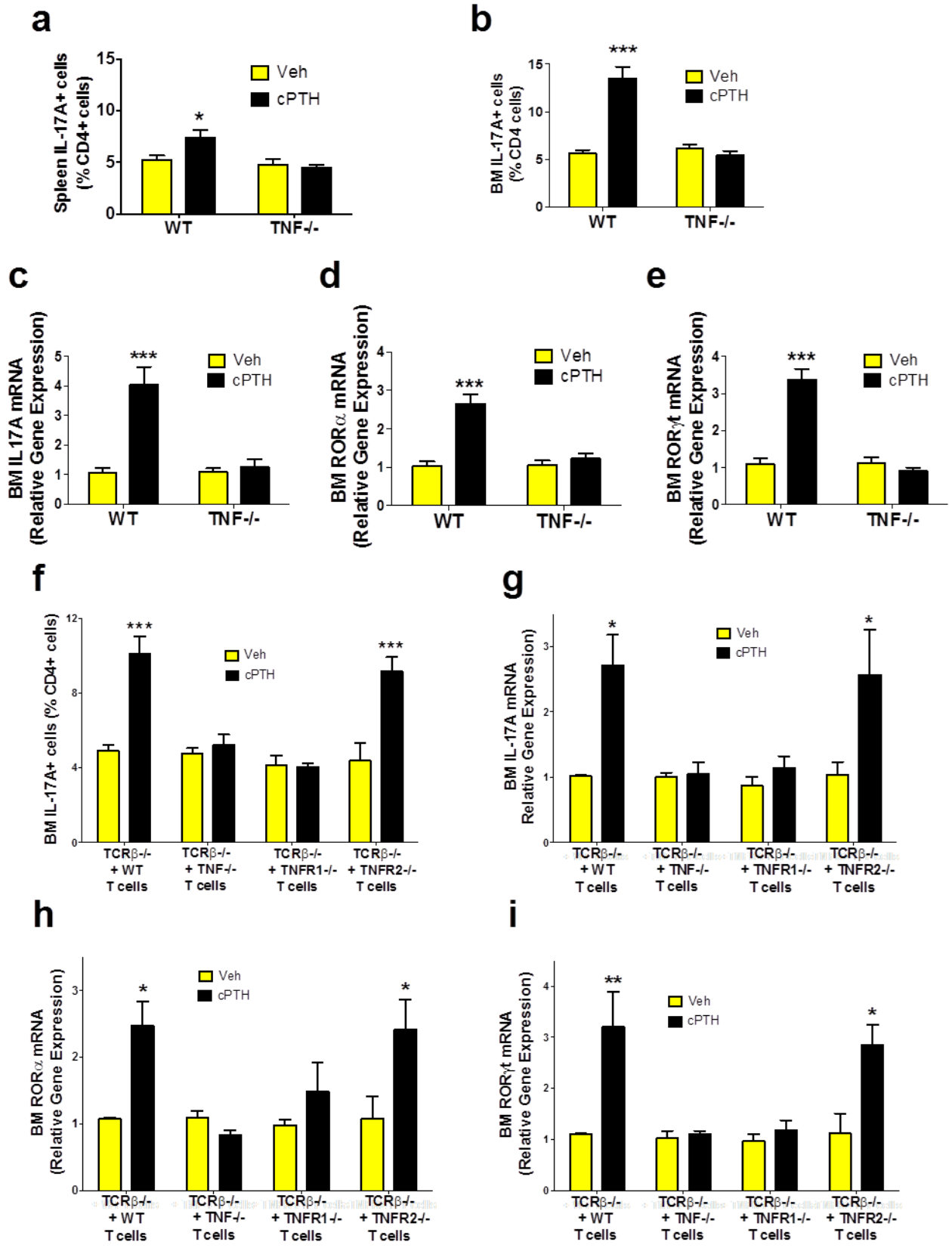
a
Spleen IL-17A+ cells (% CD4+ cells)
15
10
5
0
*
Veh
cPTH
WT
TNF-/-
b
BM IL-17A+ cells (% CD4 cells)
***
Veh
cPTH
WT
TNF-/-
c
BM IL17A mRNA (Relative Gene Expression)
***
Veh
cPTH
WT
TNF-/-
d
BM RORα mRNA (Relative Gene Expression)
***
Veh
cPTH
WT
TNF-/-
e
BM RORγt mRNA (Relative Gene Expression)
***
Veh
cPTH
WT
TNF-/-
f
BM IL-17A+ cells (% CD4+ cells)
12
8
4
0
***
***
Veh
cPTH
TCRβ-/- + WT T cells
TCRβ-/- + TNF-/- T cells
TCRβ-/- + TNFR1-/- T cells
TCRβ-/- + TNFR2-/- T cells
g
BM IL-17A mRNA Relative Gene Expression
*
*
Veh
cPTH
TCRβ-/- + WT T cells
TCRβ-/- + TNF-/- T cells
TCRβ-/- + TNFR1-/- T cells
TCRβ-/- + TNFR2-/- T cells
h
BM RORα mRNA (Relative Gene Expression)
*
*
Veh
cPTH
TCRβ-/- + WT T cells
TCRβ-/- + TNF-/- T cells
TCRβ-/- + TNFR1-/- T cells
TCRβ-/- + TNFR2-/- T cells
i
BM RORγt mRNA (Relative Gene Expression)
**
*
Veh
cPTH
TCRβ-/- + WT T cells
TCRβ-/- + TNF-/- T cells
TCRβ-/- + TNFR1-/- T cells
TCRβ-/- + TNFR2-/- T cells

Figure 5. cPTH expands Th17 cells, causes bone loss and stimulates bone resorption through activation of GαS in naïve CD4+ cells. **a.** cPTH increases the sensitivity to TNF of naïve CD4+ cells from WT and GαS fl/fl mice but not of those from GαSΔCD4,8 mice. Naïve CD4+ cells were sorted from vehicle and cPTH treated mice and cultured with TNF (10-50 ng/ml) to induce their differentiation into Th17 cells. **b**. TNFR1 mRNA levels in BM CD4+ cells. **c**. TRAF2 mRNA levels in BM CD4+ cells **d.** Frequency of BM Th17 cells. **e-g**. μCT indices of bone volume and structure. **h-j**. Serum levels of CTX, P1NP and osteocalcin (OCN). Data are shown as mean + SEM. n = 5 mice per group for panels b-c. n = 16 GαS fl/fl mice per group and 21 GαSΔCD4,8 mice per group for panels d-j. All data passed the Shapiro-Wilk normality test and were analyzed by 2-Way ANOVA. *=$p<0.05$, **=$p<0.01$, ***=$p<0.001$ and ****=$p<0.0001$ compared to the corresponding vehicle group. # = $p<0.05$ compared to the GαSΔCD4,8 cPTH group.

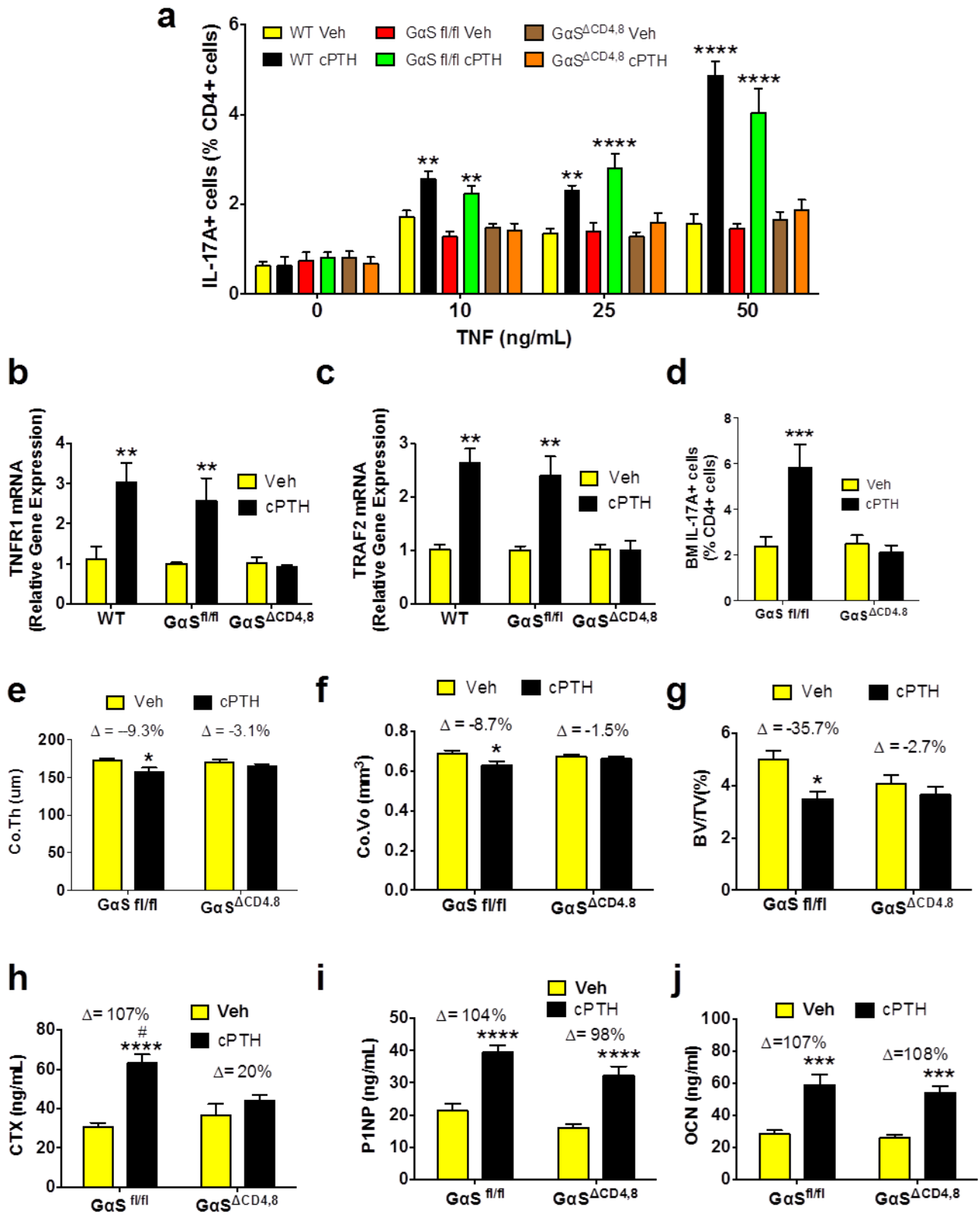
a
WT Veh
WT cPTH
GαS fl/fl Veh
GαS fl/fl cPTH
GαS ΔCD4,8 Veh
GαS ΔCD4,8 cPTH
IL-17A+ cells (% CD4+ cells)
TNF (ng/mL)
b
TNFR1 mRNA (Relative Gene Expression)
Veh
cPTH
WT
GαS fl/fl
GαS ΔCD4,8
c
TRAF2 mRNA (Relative Gene Expression)
d
BM IL-17A+ cells (% CD4+ cells)
e
Co.Th (um)
Δ = –9.3%
Δ = -3.1%
f
Co.Vo (mm3)
Δ = -8.7%
Δ = -1.5%
g
BV/TV(%)
Δ = -35.7%
Δ = -2.7%
h
CTX (ng/mL)
Δ= 107%
Δ= 20%
i
P1NP (ng/mL)
Δ= 104%
Δ= 98%
j
OCN (ng/ml)
Δ=107%
Δ=108%

Figure 6. Effects of in vivo treatment with the L-type calcium channel blocker diltiazem (DIZ) on the relative frequency of BM Th17 cells and indices of bone volume, structure and turnover in mice treated with vehicle or cPTH. **a** relative frequency of BM Th17 cells, **b** IL-17A mRNA levels in BM CD4+ cells **c-d** expression of RORα and RORγt mRNA in BM CD4+ cells, **e-j** μCT indices of bone volume and structure. **k,l.** Serum levels of CTX and P1NP. Data are shown as mean + SEM. n = 12 mice per group. All data passed the Shapiro-Wilk normality test and were analyzed by 2-Way ANOVA. *=p<0.05, **=p<0.01, ***=p<0.001 and ****=p<0.0001 compared to the corresponding vehicle group. ## = p<0.01 compared to the DIZ cPTH group.

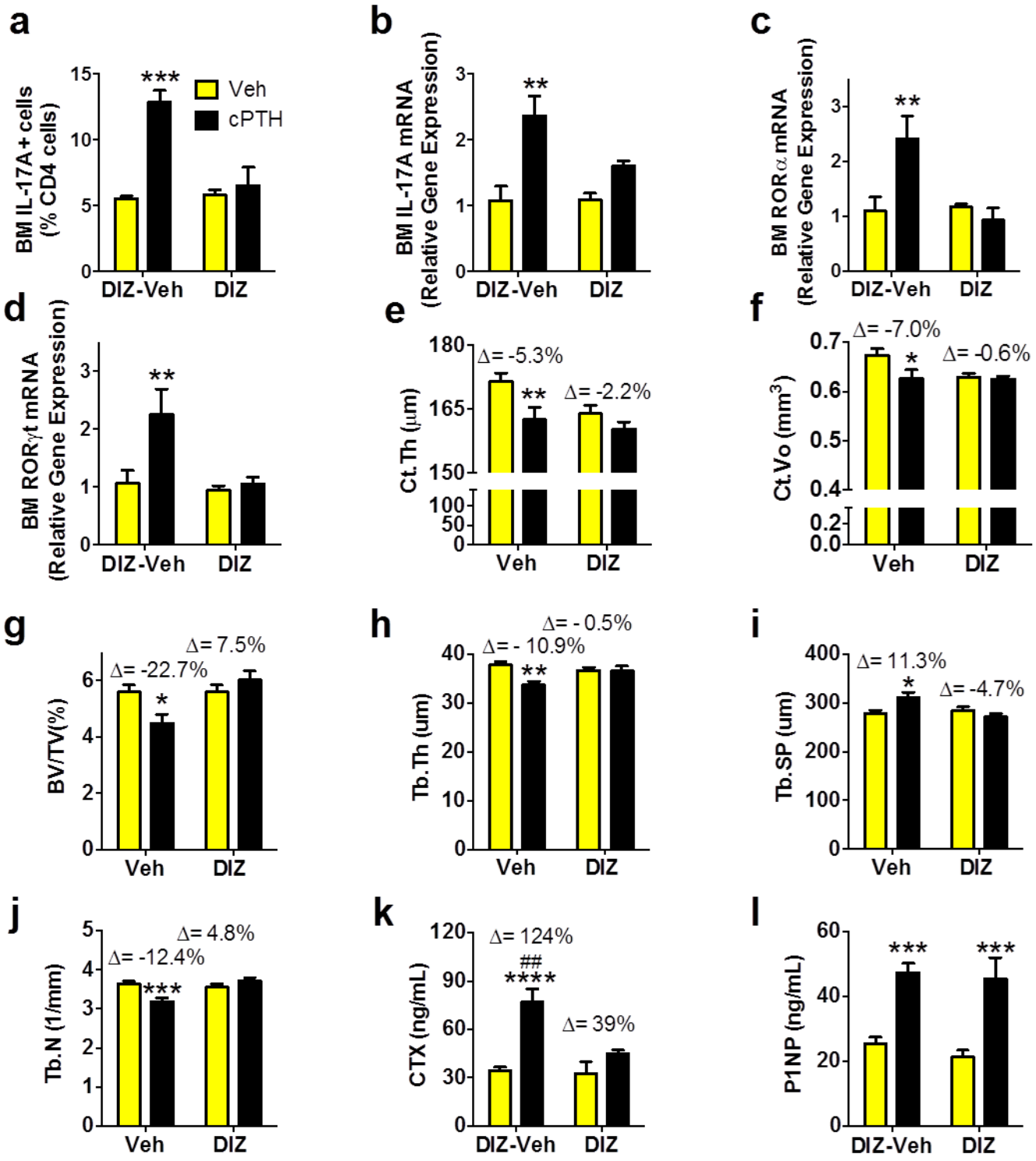
a
BM IL-17A+ cells (% CD4 cells)
Veh
cPTH
***
DIZ-Veh
DIZ
b
BM IL-17A mRNA (Relative Gene Expression)
**
c
BM RORα mRNA (Relative Gene Expression)
d
BM RORγt mRNA (Relative Gene Expression)
e
Ct.Th (μm)
Δ= -5.3%
Δ= -2.2%
Veh
f
Ct.Vo (mm3)
Δ= -7.0%
Δ= -0.6%
g
BV/TV(%)
Δ= -22.7%
Δ= 7.5%
h
Tb.Th (um)
Δ= - 10.9%
Δ= - 0.5%
i
Tb.SP (um)
Δ= 11.3%
Δ= -4.7%
j
Tb.N (1/mm)
Δ= -12.4%
Δ= 4.8%
k
CTX (ng/mL)
Δ= 124%
##
****
Δ= 39%
l
P1NP (ng/mL)

Table 1. Demographic and clinical data of healthy controls and PHPT patients before and after surgery. Data are shown as Mean + SEM for normally distributed variables (serum P and demographic data) and median with interquartile range for non-normally distributed variables (serum Ca, PTH, and 25OH Vitamin D). Values in squared parenthesis denote normal range.

	Healthy Controls	PHPT before surgery	PHPT after surgery
Study Participants (n)	57	20	20
Age (years)	60.1 ± 2.3	57.3 ± 3.4[a]	57.3 ± 3.4[a]
Males (n)	25	4	4
Males Age (years)	66.5 ± 3.6	67.5 ± 7.2[a]	67.5 ± 7.2[a]
Females (n)	32	16	16
Female Age (years)	56.7 ± 2.9	54.5 ± 3.7[a]	54.5 ± 3.7[a]
Postmenopausal females (n)	23	8 [a]	8 [a]
Years since menopause	15.5 ± 2.3	15.7 ± 3.5[a]	15.7 ± 3.5[a]
Serum Ca (mg/dL) [8.8-10.4 mg/dL]	9.4 (9.1-9.7)	10.8 (10.5-12.0)[b]	8.8 (8.7-9.1)[d,b]
Serum P (mg/dL) [2.5-4.5 mg/dL]	3.3 ±0.07	2.7 ± 0.3 [c]	3.5 ± 0.4[e,a]
PTH (pg/mL) [10-65 pg/mL]	53 (32-63)	102 (79-161)[b]	56.5 (41.8-75.8)[d,a]
25OH vitamin D [30-100 ng/mL]	19.6 (5.7-27.2)	17.8 (15.1-22.4)[a]	23.6 (21.9-30.4)[f,a]

p values: a= ns, b= <0.0001 and c=0.005 compared to Healthy Controls; d= <0.0001, e<0.05 and f <0.01 compared to PHPT.

Supplementary Table 1. The table shows the results of GLM for baseline IL17A mRNA levels (dependent variable) and disease (PHPT or control) without (crude) and with (adjusted) correction for age and gender and their interaction (*). The table shows the regression coefficient (t), the 95% confidence of interval (CI) and the p-values (p). The regression model was performed using a logarithmic transformation of baseline IL-17A mRNA levels (77 subjects were included).

	Crude analyses			**Adjusted analyses^**		
	t	**CI**	**p**	**t**	**CI**	**p**
Disease	-3.611	-1.197, -0.346	**0.001**	-3.108	-1.227, -0.228	**0.003**
Age				3.173	0.007, 0.029	**0.002**
gender				-3.03	-1.021, 0.752	0.763
Disease*gender				-2.72	-1.102, 0.837	0.786

^: Adjusted for age and gender

Supplementary Table 2. The table shows the results of GLM for baseline RORC (dependent variable) and disease (PHPT or control) without (crude) and with (adjusted) correction for age and gender and their interaction (*). The table shows the regression coefficient (t), the 95% confidence of interval (CI) and the p-values (p). The regression model was performed using a logarithmic transformation of baseline RORC mRNA levels (77 subjects were included).

	Crude analyses			**Adjusted analyses^**		
	t	**CI**	**p**	**t**	**CI**	**p**
Disease	-3.741	-0.848, -0.259	**<0.0001**	-2.848	-0.802,-0.142	**0.006**
Age				2.576	0.002,0.0018	**0.012**
gender				-0.884	-0.881,0.340	0.380
Disease*gender				-0.364	-0.790,0.546	0.717

^: Adjusted for age and gender